Confocal laser scanning microscopy: Applications in material science and technology

B V R TATA and BALDEV RAJ*

Metallurgy and Materials Group, Indira Gandhi Centre for Atomic Research, Kalpakkam 603 102, India

Abstract. Confocal laser scanning microscope (CLSM) has great advantage over a conventional microscope because it rejects the light that does not come from the focal plane, enabling one to perform optical slicing and construction of three-dimensional (3D) images. Further its high axial resolution, sharp image quality and associated quantitative image analysis provide vital structural information in the mesoscopic range for the full 3D realization of the microstructure. Because of this unique feature, CLSM is now finding wider applications in the study of variety of materials and processes such as phase separation in binary polymer mixtures, fracture toughness in alloys, in determining residual strains in fibre-reinforced metal composites, and in microvisualization of corrosion. This paper reviews some of these recent applications and also discusses our results on colloidal dispersions. CLSM has been used to characterize the amorphous structure in highly-charged colloidal systems which have undergone gas–solid transition. CLSM images show presence of large voids deep inside the disordered suspensions. Frame averaged images reveal that the structural disorder is amorphous. The reasons for voids coexisting with dense amorphous regions and their implications on colloidal interactions are discussed. The article also reviews the use of fluorescence-CLSM in the investigation of novel materials of technological importance such as template-directed colloidal crystals with preferred orientations and multilayered structures with different crystal plane symmetries. Direct measurement of the interfacial curvatures for a bicontinuous polymer blend system as well as real space measurement of structure in phase separating polymer mixtures are now possible using CLSM. This paper reviews some of these results highlighting the unique advantages of confocal microscopy for better understanding of the microstructure and mechanistic aspects of various important phenomena in a large variety of materials.

Keywords. Confocal laser scanning microscope; optical microscopy; colloidal suspensions; structural ordering; gas–solid transition; colloidal crystals; phase separation; polymer mixtures; alloys; composites; fracture; corrosion; residual strain.

1. Introduction

Conventional microscopes have been in use in various areas of research for a long time. The recent advancements in video microscopy and digital imaging techniques have enhanced the capabilities of these microscopes, thereby providing powerful investigative tools. The information from these instruments has largely remained as two-dimensional (2D). Thus, there is a requirement for three-dimensional (3D) information, for example in stereology, and life sciences. Stereologists use histological sections to generate 3D information (Howard 1990), wherein physical sections are used either serially to recreate third dimension or in pairs to form a 3D probe. But these methods necessarily destroy the specimen as part of preparative work, hence multiple sampling opportunities are restricted. With the advent of confocal laser scanning microscope (CLSM), new horizons for quantitative

microscopy have opened up and it is now available as nondestructive 3D probe (Wilson 1990). Since the light that does not come from the focal plane is rejected by CLSM, it enables optical slicing and construction of three-dimensional images. Consequently, the same specimen can be subjected to multiple investigations either in a time series or with different geometrical probes or single probe from a number of orientations. This approach has paved a way for investigating new advances in stereology.

The recent developments in powerful but low-cost computer data processing and imaging systems along with the availability of laser light sources have helped in popularizing the CLSM in the field of life sciences, and semiconductor device technology. Since these instruments give high-contrast images, their output can be subjected for further image analysis. The three-dimensional data sets, which otherwise have not been available through conventional microscopes, have created interest in large number of research groups to develop

---

*Author for correspondence

image processing algorithms which cater to specific applications. The availability of such data sets provide for three-dimensional studies in the field of spatial statistics, and to obtain zero-dimensional quantities. For example, the zero-dimensional property of immense interest is connectivity. In biology, the connectivity of neurons in the central nervous system is a key parameter and in the field of petrology, connectivity of pore spaces in sand stone rocks is of major interest. Confocal microscopes provide such connectivity data (Howard 1990). Since these instruments can operate both in bright field as well as in fluorescence mode, these are extensively used to image thick biological samples in three dimensions.

Optical microscopy coupled with digital video imaging techniques (Kepler and Fraden 1994; Kesavamoorthy et al 1991; Crocker and Grier 1996a, b; Grier and Murray 1996) and CLSM have been extensively used to probe structural ordering and dynamics in charge-stabilized colloidal suspensions (Dosho et al 1993; Ito et al 1994; Yoshida et al 1995; Ise et al 1996; Muromoto et al 1997; Tata et al 1997a). Crystalline order of polystyrene suspensions with interparticle distances of the order of microns has been investigated using optical microscopy (Kesavamoorthy et al 1991; Tata 1992) with an aim to analyze structure in real space. Conventional microscope with an oil immersion type objective gives a magnification of about 1250 × and the attached video camera can record image of a frame within 40 ms. Video frame grabber records the particle positions and micrographs can be obtained using the stored image in the memory

of the image processor. Figure 1 shows the micrographs of 0·53 μm diameter polystyrene particles dispersed in deionized water medium, using such an optical microscopy set up (Kesavamoorthy et al 1991). The 2D-crystalline order in the first layer (figure 1a) is very clear while the fourth layer (figure 1b) has very poor contrast. The interlayer distance is ~ 3 μm. The poor contrast arises due to the scattering from other layers. Complete loss of contrast was observed beyond a distance of ~ 12 μm from the cover-slip (Kesavamoorthy et al 1991; Tata 1992). Thus, conventional optical microscopy has strong limitations both for depth resolution as well as image quality and therefore can not be used for structural analysis of bulk suspensions. We have shown that CLSM obviates these limitations as well as serves as an excellent probe for analyzing structure of bulk colloidal crystals.

This article describes the principle of a simple confocal microscope, the types of scanning mechanisms that are conventionally employed and different modes of operation. In highly charged colloidal systems, CLSM is also useful in characterizing the amorphous structure and in identifying the gas–solid coexistence in deionized suspensions. Currently these suspensions are studied with great interest as these exhibit various phases found in condensed matter and have helped in understanding the fundamental processes such as crystallization and glass formation. The applications of CLSM in studying processes such as phase separation in binary polymer mixtures, fracture toughness in alloys, in determining residual strains in fibre-reinforced metal composites and corrosion
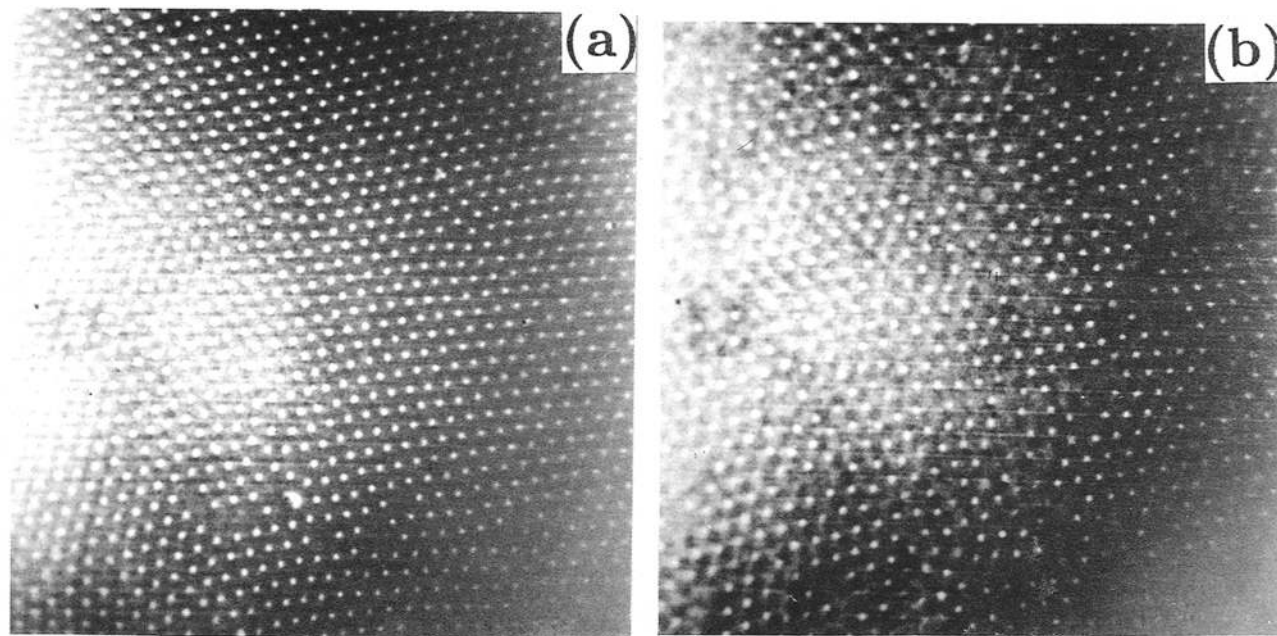
Figure 1. Micrographs showing 2D crystalline order in bulk suspension of polystyrene particles of 0·53 μm diameter; (a) the first layer (layer close to the coverslip) and (b) the fourth layer (~ 12 μm from the coverslip) (Kesavamoorthy et al 1991).

in metals are also presented. Although confocal microscopes are increasingly used in life sciences and biology, such applications are not covered primarily due to inadequacy of the authors expertise.

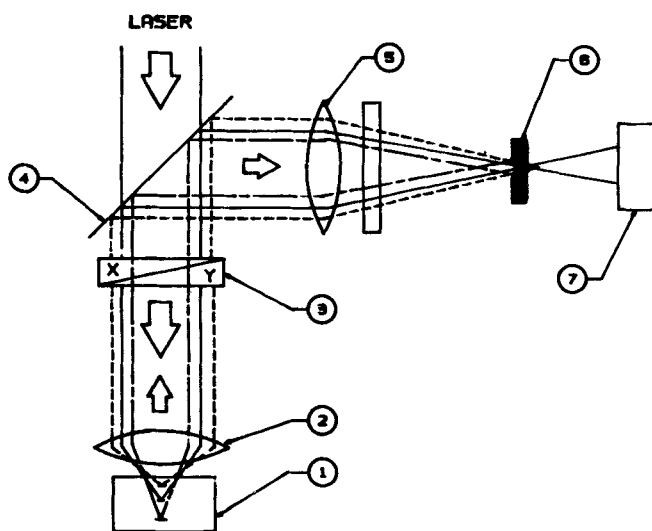## 2. Principle and types of confocal microscopes

Before we describe the confocal principle, it is important to know about the advantages of choosing a scanning approach which is inherent in all confocal scanning microscopes. The optical components of a conventional microscope have severe requirement on optics, since the microscope functions as a parallel processing system which images the entire object field simultaneously. The scanning approach however relaxes this requirement on optics, as image of the entire object field is built not simultaneously but by scanning and imaging only one object point at a time. Further, it gives the freedom to modify the optical system in simple ways to exploit fully the potential of the confocal mode and other imaging modes. The basic principle of a confocal microscope is easy to understand despite complicated electronic, mechanical and optical systems associated with the commercial instruments. Figure 2 illustrates the principle of a simple reflection mode CLSM (Wilson 1990; Dixon 1996). When a pinhole is illuminated by laser or any other light source, light emerging out from the pinhole passes through a beam splitter and is focussed by an

Figure 2. Schematic optical layout of reflection mode confocal laser scanning microscope. (1) sample, (2) objective lens, (3) XY-scanner, (4) beam splitter, (5) focusing lens, (6) pinhole and (7) detector (photo-multiplier tube). The depicted beam paths show that light scattered from any other position on the sample, including those above or below the focal plane, is rejected by the pinhole which acts as spatial filter. The illuminated pinhole is not shown in the figure.

objective lens to a spot in the focal plane, where the sample is placed. Light reflected from this spot is partly reflected by the beam splitter towards the pinhole in front of the detector. Light reflected from any other parts of the sample, including parts above or below the focal plane, reach the edge of the detector pinhole and are not detected by the detector. The objective lens forms an image of the detector pinhole and the illuminating pinhole at the same spot in the focal plane, hence these are said to be confocal with each other. The selective rejection of light is responsible for formation of sharp images and increased depth resolution of confocal microscopes. This depth discrimination property is the major reason for the advantages of the confocal microscopes.

The image of certain portion of the sample using CLSM is obtained either by moving the specimen under a stationary focussed beam ('scanning stage' microscope) or by scanning the beam using mechanical mirrors so that the focussed spot moves across the specimen ('scanning beam' microscope). Though scanning stage microscopes are relatively slow and usually have the problem of mechanical vibrations, they have the advantage of simple optical system, and produce good images without the loss of resolution and contrast at the edge of the field. Since it is possible to have identical resolution and contrast across the entire field of view irrespective of the magnification, even low-magnification images can be taken with high numerical aperture (NA) objectives. This particular advantage is exploited in fluorescence microscopy where high aperture also implies greater signal collection level. The ability to scan slowly is also an advantage in the case of fluorescence microscopy (Wilson 1990).

Situations where speed is important, beam-scanning approach is employed. The scanning is achieved by using vibrating galvanometer-type mirrors or rotating mirror wheels or acousto-optic beam deflectors. Since each point on the specimen is illuminated only for a very short time, high beam intensity is necessary, hence, lasers are used as the source of light. This is also true for scanning stage microscopes. The optical system is usually complex in scanning beam microscopes. Unlike in scanning stage microscopes, the magnification is coupled with resolution, hence it is necessary to change objective lenses to cover the entire magnification range. The major advantage of a scanning beam system is that it is usually built around conventional optical microscope, which permits binocular viewing to locate the region of interest.

The serious disadvantage of the approaches mentioned above is the need to use television screen to see an image. Much more convenient system, which allows to view the confocal image directly by eye in real time, is the tandem scanning confocal microscope. This microscope adopts a different scanning procedure than

those mentioned above. In these the spot across the specimen is scanned by moving the illuminating pinhole and synchronizing the movement of detector pinhole with it. Further, a large number of pinholes are used on a disk with which the instrument acts like several hundred confocal microscopes all working in parallel. The disk is rotated at high speed to produce a flicker-free image of the entire field of view. Great care is taken in choosing the size and spacing of the pinholes in the disk. Such a tandem scanning microscope provides a real-time confocal image, which can be viewed through an eyepiece (Kino and Xiao 1990). While these microscopes work well on highly reflecting specimens as only a small percent of the light from the source passes through the disk, weakly reflecting and fluorescent specimens look dim. Nevertheless, these can produce good images with the help of image intensifiers (Boyde *et al* 1990).

There is also considerable interest in forming an image which depends on the differences in phase or amplitude. Differential amplitude contrast confocal microscopes as well as differential phase contrast microscopes which provide optical sectioning and depth discrimination property have also been in use, which have been reviewed earlier (Wilson 1990).

3. Applications in soft condensed matter

In this section we present some of the applications of confocal scanning microscopes in investigating the condensed matter systems, including colloidal systems and polymer mixtures.

3.1 *Colloidal systems*

Charge-stabilized (Sood 1991; Arora and Rajagopalan 1996) as well as sterically-stabilized colloidal (Pusey and van Megen 1986, 1987; van Megen 1995; Arora and Tata 1998) suspensions are studied for their technological applications such as optical devices (Asher *et al* 1986; Chang *et al* 1994; Sunkara *et al* 1994) and materials with photonic band gaps (Tarhan and Watson 1996). Colloidal dispersions of monodisperse spheres form colloidal crystals with lattice constant of the order of the wavelength of light, allowing light scattering, small-angle and ultra-small-angle X-ray scattering (USAXS) and optical microscopy (Arora and Tata 1998) to probe the structure. The characteristic time scales for colloidal crystallization process are also easily accessible, and the interaction between particles can be tuned by selecting an appropriate combination of surface treatment and solvent in sterically-stabilized suspensions, and by controlling the charge on the particles and the salt concentration in charge-stabilized suspensions. In addition to the crystalline order, colloidal dispersions also exhibit structural ordering similar to those found in atomic

liquids and glasses. These features and the striking closeness of magnitudes of the molar elastic constants, latent heat of melting and other thermodynamic parameters make these as simple and convenient model systems for fundamental studies on crystallization, melting and glass formation (Pusey and van Megen 1986, 1987; van Megen 1995; Arora and Tata 1996). The colloidal crystals have elastic constants $\sim 10^{10}$ dynes/cm^2, which make these extremely fragile as well as provide best example of a soft condensed matter system. Phenomena that have been studied using such systems include the kinetics of crystallization (Schätzel 1996), melting (Arora and Tata 1996), vapour–liquid condensation (Tata *et al* 1992; Tata and Arora 1996) and the phase diagrams involving body-centred cubic (bcc), face-centred cubic (fcc) structures, fluid and glassy phases (Sirota *et al* 1989; Sood 1991).

3.2 *Disordered suspensions*

Colloidal particles (e.g. polymethylmethacrylate, silica etc), with a thin layer of polymer, when dispersed in suitable organic solvents, interact with steep repulsive forces and serve as model hard-sphere systems (Pusey and van Megen 1986, 1987). Presence of free polymer molecules results in a depletion attraction which is of relatively short range (Lekkerkerker *et al* 1992; Ilett *et al* 1995; Arora and Tata 1998). On the other hand, polymer latex particles with dissociable end groups, when dispersed in a suitable dielectric medium like water, acquire a large negative charge of the order of few hundred electronic charges. These charge-stabilized dispersions interact strongly with electrostatic interactions (Sood 1991; Arora and Rajagopalan 1996). Purely repulsive screened Coulomb interaction was believed to be responsible for freezing of the Brownian motion of the particles, leading to appearance of crystalline order in these suspensions. However, the observations such as vapour–liquid condensation (Tata *et al* 1992; Tata and Arora 1996), reentrant transition (Arora *et al* 1988; Tata and Arora 1996), existence of metastable colloidal crystals (Larsen and Grier 1996, 1997) and non-space filling nature of the suspensions (Ise *et al* 1996), suggest the existence of long-range attraction in the interparticle interaction of these suspensions. This has renewed interest in investigating the pair-potential, both theoretically (Sogami and Ise 1984, Tata and Arora 1995; Chu and Wasan 1996; Rajagopalan 1996; van Roij and Hansen 1997) as well as experimentally (Kepler and Fraden 1994; Crocker and Grier 1996b; Tata and Ise 1998). We have reviewed some of our experimental investigations carried out using CLSM to probe the internal structure of highly-charged colloidal suspensions which suggest the existence of attraction and confirm the predictions of Monte-Carlo (MC) simulations carried out as a function of charge density σ (Tata and Ise 1996).
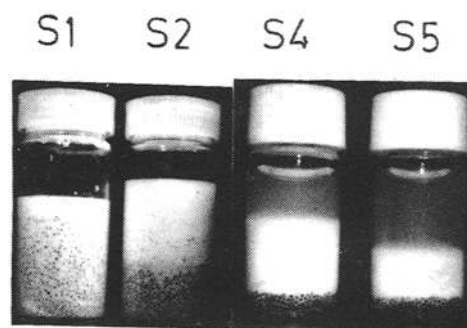
Highly-charged poly chlorostyrene styrene sulfonate (PCSS) particles, diameter, d, 180 nm and charge density, σ, 0·25 $\mu C/cm^2$, in aqueous medium were synthesized using emulsifier-free copolymerization method. The sufficient electron density difference (contrast) of these suspensions helps to perform USAXS studies (Matsuoka and Ise 1993; Ise et al 1996; Tata et al 1997a). Samples with volume fractions, ϕ, ranging over two orders of magnitude (see table 1), have been investigated under completely deionized conditions. Suspensions with $\phi > 0·005$ appeared homogeneous for an unaided eye (see photographs of samples S0 and S1 in figure 3) and did not show iridescence. However, samples with $\phi < 0·005$ showed macroscopic phase separation (see photographs of samples S5 and S6 in figure 3) as dense and rare phase regions. The former, which settled down due to gravity, showed iridescence suggesting crystalline order. The rare phase at the top showed only very few particles. However, CLSM study on samples S0–S3 showed presence of large size voids deep inside the suspensions (see figure 4) which coexisted with disordered dense regions of particles (Tata et al 1997a). These voids were found to have only a few colloidal particles. Averaging of the image frames over several seconds improved the sharpness of the image (see figure 5), suggesting that the disordered dense regions were amorphous. The split second peak in the structure factor measured using USAXS apparatus also confirmed the existence of glass-like structure within the dense regions (Tata et al 1997a). The USAXS profiles did not contain any signature of voids, nevertheless the first peak was found to have shifted to higher Q side, where Q is the scattering vector. CLSM observations confirmed the presence of voids deep inside the suspensions. Most of the voids are found to be spherical from the analysis of confocal images obtained as function of depth, z (see figure 6) (Tata and Ise 1997). It may be mentioned here that when the voids are large (about 30–70 μm) and also polydisperse in size, the interpretation of scattering data is not straightforward. However, confocal microscopy allows direct observation and easy determination of size, shape and polydispersity of large size structural inhomogeneities in highly turbid samples.

The interparticle separation D_{exp} within the amorphous dense regions obtained from USAXS profiles, is found to be smaller than the average interparticle distance, (D_0), calculated from the particle concentration (Tata et al 1997a). The observation of amorphous dense phase together with voids provides evidence for gas–solid coexistence, suggesting existence of long-range attraction in the interparticle interaction. The volume occupied by the voids increases with dilution. Below a volume fraction of 0·005, the void fraction (i.e. volume occupied by voids) is sufficiently high and voids coalesce, leading to macroscopic phase separation in samples S4–S6. Further, the dense phase is expected to appear in the form of clusters during phase separation, which will settle down due to gravity as density of colloidal particle is larger than the density of water.

It is known that gas–solid transition in atomic systems is owing to van der Waals attraction. In order to know whether an effective pair potential $U_s(r)$, having a long-range attractive term, leads to such a gas–solid transition in charge-stabilized suspensions, Tata et al (1997b) performed computer simulations for the measured suspension parameters to understand the experimental observations. It may be mentioned here that $U_s(r)$ has been derived by Sogami for macroionic suspensions of finite volume fraction. Figure 7 shows Monte-Carlo simulation results for different volume fractions. At high volume fractions, a crystalline order is seen which undergoes a gas–solid transition upon lowering of ϕ. The first peak height in the structure factor, S_{max}, obtained from simulations has been used to identify the transition. The transition takes place at a volume fraction of 0·1 (see figure 8). A good agreement between simulations and experimental observations has been reported (Tata et al 1997a, b). The results are understood on the basis of the behaviour of $U_s(r)$ as function of ϕ. Since the charge density of these particles is high, the corresponding

Table 1. Sample labels and volume fractions.

| Sample	ϕ
S0	0·0595
S1	0·0244
S2	0·0122
S3	0·0061
S4	0·0031
S5	0·0020
S6	0·0008

Figure 3. Photographs of sample cells showing fully deionized PCSS suspensions S1, S2, S4 and S5. Suspensions S1 and S2 remained homogeneous and did not exhibit iridescence. Suspensions S4 and S5 exhibited the dense phase (lower part of the cell) macroscopically separated from the very dilute phase (upper part of the cell). The dense phase showed iridescence. Ion-exchange resin was at the bottom of the cell.

well depths of $U_s(r)$ are quite large ($> 6.5k_BT$) and the well positions are also less than D_0 (Tata *et al* 1997a). Hence the particles experience strong attractive forces arising from the large well depths leading to formation of disordered dense regions and voids (see figure 7b).

At very low volume fractions ($\phi < 0.005$), the volume occupied by the voids is more than that occupied by the particles and dense phase is expected to appear in the form of clusters as seen in simulations (figure 7c). Clusters can be observed in a density-matched suspension. Density matching is done by dispersing the particles in

a medium whose density is same as that of the colloidal particles. Suspensions containing such clusters are usually turbid for light scattering studies and do not have good contrast for USAXS studies. However, when the density-matched suspensions were investigated using CLSM, Tata *et al* (1997b) observed formation of clusters (figure 9) at low volume fractions; consistent with MC simulation results. The density matching is done using a 60% glycerol aqueous solution. It may be mentioned here that the occurrence of gas–solid transition and vapour–liquid transition can also be understood using a
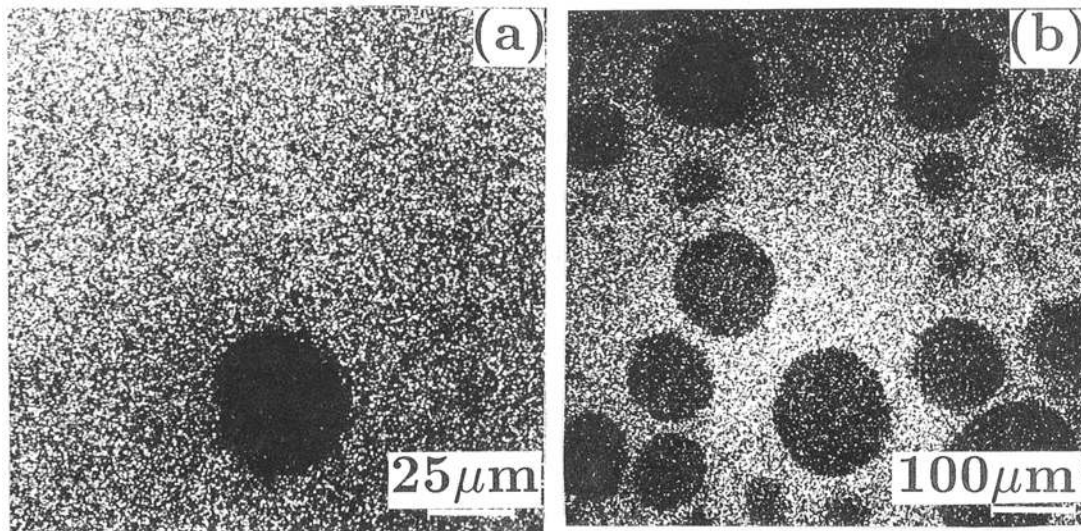

Figure 4. CLSM micrographs showing voids (black regions) and disordered dense regions (white regions) for suspension with (a) $\phi = 0.0244$ at a distance of 46 μm from coverslip using an objective lens $40 \times /0.75$ and (b) $\phi = 0.0061$ at a distance of 96 μm from coverslip objective lens $20 \times /0.5$.
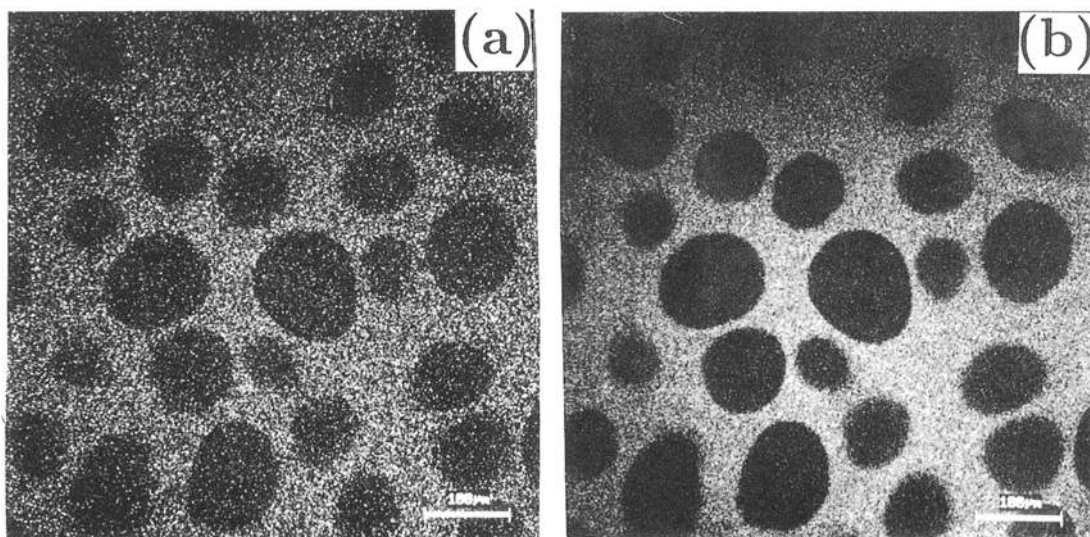

Figure 5. CLSM micrographs for suspension with $\phi = 0.0061$ at a distance of 76 μm from coverslip using an objective lens $20 \times /0.5$ (a) single frame (scan time 1.08 s) and (b) averaged over 16 frames. Frame averaging greatly improves the sharpness of the image, suggesting diffusion of particles is negligibly small within the observation time.
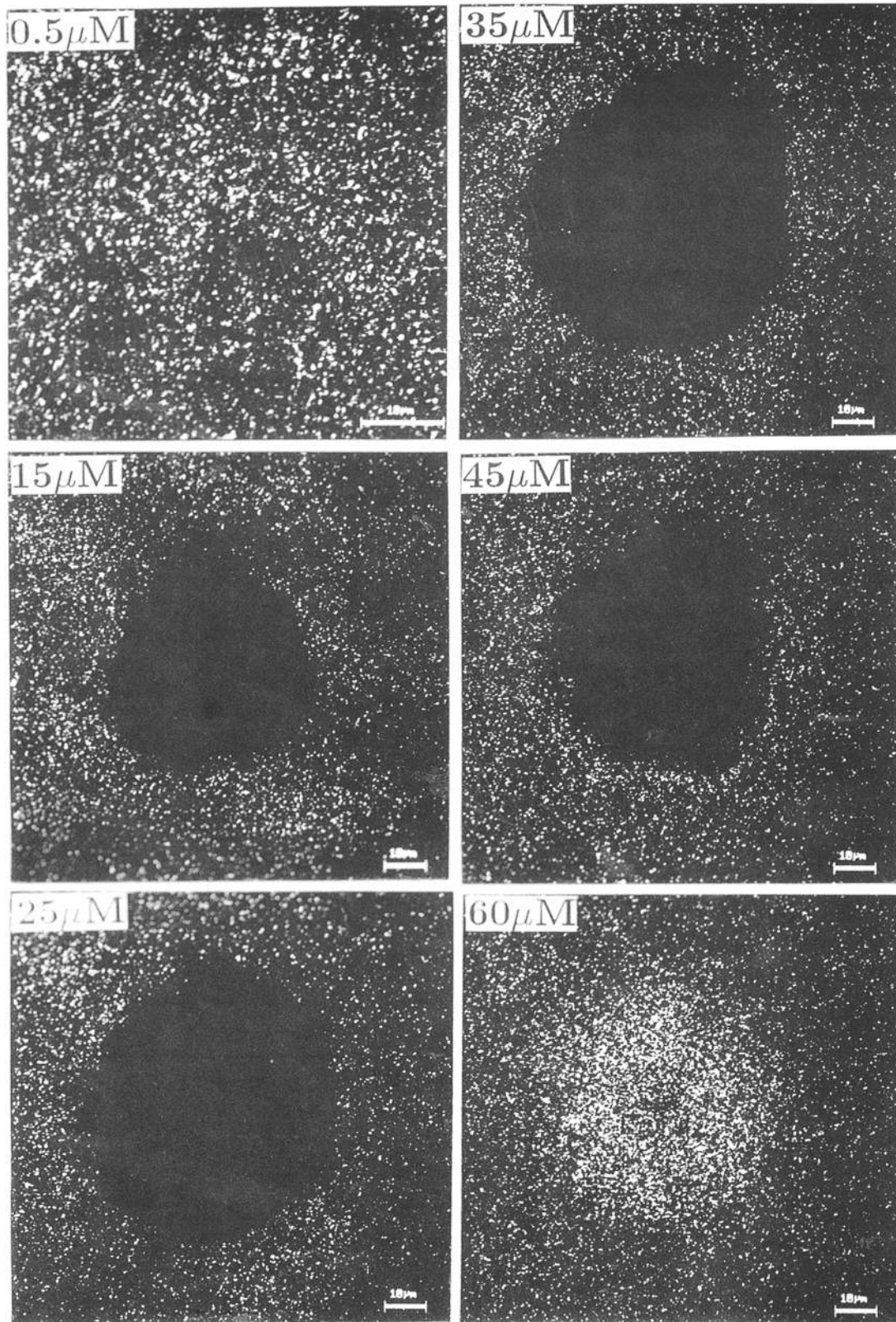
Figure 6. CLSM micrographs of optical slices taken at different z-distances from coverslip of void in a suspension with $\phi = 0.0244$ using an objective lens $40 \times /0.75$. Wavelength of the laser is 647 nm, bar = 10 μm.
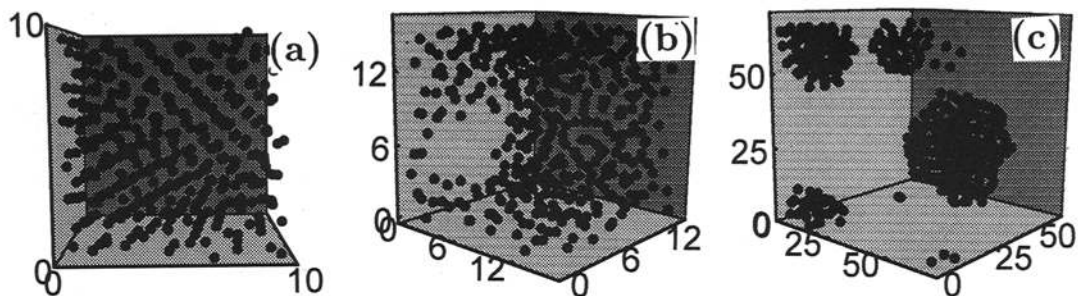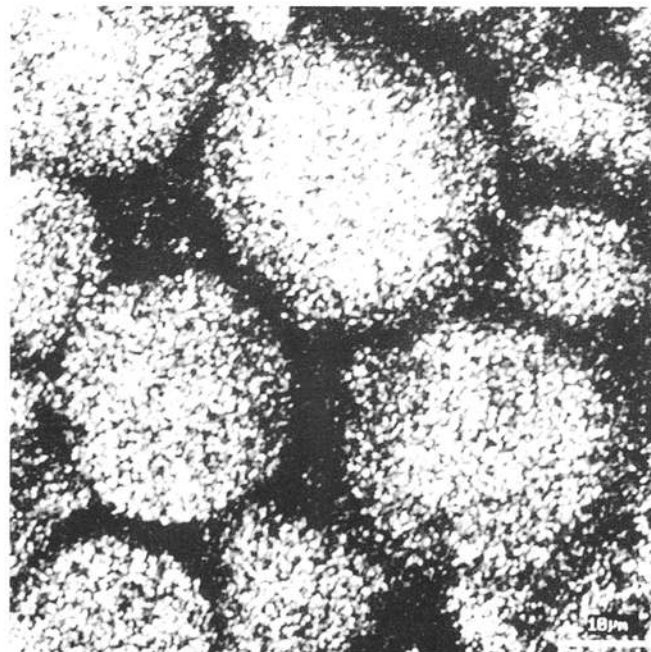
Figure 7. 3D plots of particles in MC cell corresponding to suspensions with (a) $\phi = 0.25$, (b) 0.0595 and (c) 0.0008. The other suspension parameters used in the simulations are same as that measured experimentally (Tata *et al* 1997a). Notice the crystalline order at $\phi = 0.25$, coexistence of void with disordered structure at $\phi = 0.0595$ and dense particle clusters at $\phi = 0.0008$.
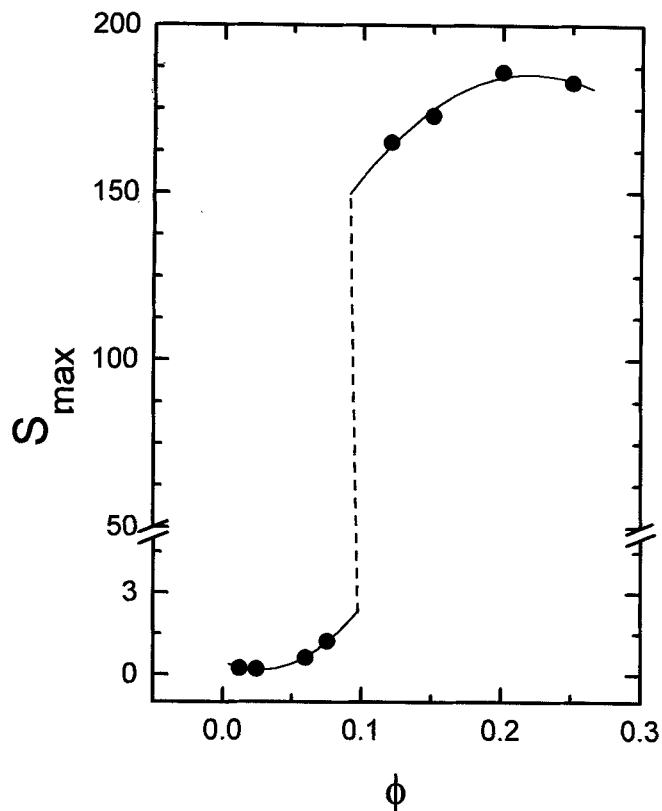
Figure 8. S_{max} obtained from MC simulations is shown as function of ϕ. The sharp fall in S_{max} at $\phi \sim 0.1$ indicates the occurrence of gas–solid transition in highly-charged suspensions.

Figure 9. CLSM micrograph showing dense particle clusters in a density-matched deionized PCSS suspension with $\phi = 0.002$ consistent with MC simulation results (see figure 7c). Objective lens used has magnification of $40 \times /0.75$. Wavelength of the laser is 647 nm, bar = 10 μm.

purely repulsive pair-potential, provided the effective Hamiltonian contains an attractive term which can drive a spinodal instability (van Roij and Hansen 1997). However, the agreement between the results obtained using this effective Hamiltonian and the experimental results is yet to be demonstrated.

Recently, Muromoto *et al* (1997) used CLSM to investigate the effect of similarly-charged glass plate on

the distribution of negatively-charged colloidal particles as a function of distance from the glass plate with an aim to understand the plate–particle interaction and the role of charge on the glass plate. The surface potential of the negatively-charged glass surface is varied over a wide extent (− 4 mV to − 94 mV) by varying the ionic strength of the solution as well as by polymerizing charged or uncharged monomers to reactive end groups of silane coupling agents bound to SiOH groups on the glass surface. The particles were observed using a reversed-type CLSM (LSM410, Carl Zeiss), using an objective lens of 40 × and working distance of 330 μm.

The depth resolution of this microscope with this optical system is about 2–3 μm. Particles within an image frame ($40 \times 40\ \mu m^2$) are counted using a digital image processor. Particle distribution profiles as a function of distance z from the glass surface are measured from the images stored at different distances. These profiles show more number of particles close to the wall ($< 10\ \mu m$) compared to the particles further away from the wall, implying gathering of negatively-charged particles close to the similarly-charged glass plate. The gathering is found to be more when the glass plate is highly charged and no such gathering is reported when the glass plate is less charged. These results also suggest that there exist an effective long-range attraction in the plate–particle interaction (Muromoto et al 1997). The origin of attraction is expected to be similar to that observed in bulk charge-stabilized suspensions.

3.3 Ordered suspensions

Crystalline order appears in deionized charged suspensions even at low volume fraction ($\phi < 0.001$). Whereas, sterically-stabilized suspensions, such as silica particles dispersed in a polar solvent, crystallize in close-packed structures at high volume fractions (Pusey and van Megen 1986, 1987; Sood 1991; Arora and Tata 1998). Structural analysis by conventional light microscopy is not appropriate for these concentrated crystals, since the intensity of light is strongly attenuated by scattering. However by incorporating fluorescent dye in the particles, concentrated suspensions can be investigated using a fluorescence CLSM. With this it is also possible to distinguish the particles which are at a surface–surface separation smaller than the resolution of the microscope, provided the particles contain the dye within their core which is surrounded by a nonfluorescent shell. Fluorescence-CLSM has been extensively used to study dispersions of fluorescein isothiocynate (FITC)- and rhodamine isothiocynate (RITC)-labelled silica spheres (Verhaegh and van Blaaderen 1994). The powerful depth discrimination and the high resolution of fluorescence-CLSM allows the imaging of individual particles in the bulk of a concentrated suspension. In a fluorescence-CLSM, the diffraction limited point is focussed inside the specimen and the fluorescence intensity is imaged on a point detector and, consequently, the image is built by scanning. With an excitation wavelength of 488 nm for the FITC dye and lens with numerical aperture 1·3, a lateral resolution of 0·2 μm (both in x and y direction) and an axial resolution of 0·65 μm are possible. Recently Verhaegh and Blaaderen (1994) made an assessment of FITC and RITC dyed particles for their photo-bleachability using a fluorescent CLSM by examining the fluorescent intensity recorded over small region of the line scan. Their assessment reveals that the bleachability of both the fluorophores,

when incorporated in silica spheres, are comparable. Further, RITC-labelled silica spheres are found to be better than FITC-labelled particles, as the former can withstand high temperatures (473 K).

RITC-labelled stearyl-coated silica spheres dispersed in chloroform at a volume fraction of 0·07, which exhibit crystallization, have been studied using fluorescence-CLSM (Verhaegh and Blaaderen 1994). The dynamics of crystal growth process has been studied by analyzing the images which were recorded at different intervals of time after homogenizing the samples. By monitoring the crystal/liquid interface as function of time, the growth rate of crystal plane during the crystallization process is found to be about 4 μm/s. At lower volume fractions the coexistence of colloidal liquid and colloidal crystal has also been observed. A binary mixture of RITC-labelled spheres and FITC-labelled spheres dispersed in chloroform has also been studied by Verhaegh and Blaaderen (1994) both immediately after mixing and after several days of mixing. By simultaneous excitation and detection of both the fluorophores, they could record combined as well as separate images of FITC- and RITC-labelled particles. Thus fluorescence-CLSM allows direct visualization of one type of labelled particles in the bulk of other particles. Such images provide valuable structural information in real space. It is possible to obtain partial and total pair–correlation functions, which otherwise can only be obtained in computer simulations. Fourier transforming the partial and total structure factor data obtained from neutron scattering experiments yield such information of atomic systems but can not be used for colloidal systems, as the range of Q is quite different.

Stacking disorder is quite common in close-packed structures. Stacking of hexagonal close-packed (hcp) planes in the sequence ABAB... gives the hcp structure whereas the sequence ABCABC... yields fcc structure. Frankel and Ladd (1984) showed the free energy for an hcp structure of hard-sphere colloidal system as only $2 \times 10^{-3} k_B T$ per particle higher than the fcc structure. In view of this small difference, these planes are often randomly stacked giving rise to a stacking disorder. If two adjacent layers are in sequence AB, then the third layer can be in site C with stacking probability α and in site A with probability $1 - \alpha$. For fcc $\alpha = 1$ and for hcp $\alpha = 0$. $\alpha = 0.5$ corresponds to completely random stacking. The Bragg reflections of visible light, which appears as iridescence for the unaided eye, can be used to determine crystal structure of colloidal dispersions. The limitation of diffraction techniques, which provide the average structure factor in reciprocal space, is that it is hard to obtain the information about local structures such as vacancies, defects and coexistence of different phases. For using electron microscopy the samples have to be rapidly frozen. Since the rapid freezing process is expected to affect the actual structure, use of electron

microscopy is strongly limited. Turbidity hinders the use of conventional light microscopy. It is shown that direct observation and determination of stacking disorder is now possible using a fluorescence-CLSM. Verhaegh *et al* (1995) used fluorescence-CLSM (Biorad MRC 600) to observe the stacking disorder in rhodamine-labelled silica spheres dispersed in chloroform. The stacking disorder is measured in polycrystalline sample having a volume fraction of 0·07. Using a series of 13 confocal micrographs taken at axial separation of 0·4 μm at an average depth of 20 μm from the glass wall, they could determine the average stacking probability to be 0·4 ± 0·2 in the hexagonally close packed planes. These results thus demonstrate the power of confocal microscopy in direct observation and determination of stacking disorder in a randomly stacked colloidal crystal.

As mentioned earlier, the colloidal crystals are 3D periodic structures with lattice constants of the order of microns and have many technological applications. Such applications require large single crystals with adjustable crystal orientation. Van Blaaderen *et al* (1997) have recently developed a 'colloidal epitaxy process' similar to that employed for epitaxial growth of thin atomic crystalline layers on a template consisting of an oriented single crystal. A 500 nm-thick fluorescent polymer layer with holes made with electron beam lithography has been used as a template. The thickness is close to the particle radius (525 nm) of the fluorescent silica spheres. The interparticle forces are made hard-sphere-like by choosing the dispersion medium and the ionic strength of the suspension. Controlled layer-by-layer growth was achieved by slow sedimentation of the particles on the substrate. By preparing a pattern of holes matching with the (100) plane of fcc crystal, a pure crystal of several millimeters of thickness was formed. The three-dimensional stack of confocal micrographs obtained using a fluorescence-CLSM (Multiprobe 2001) has been analyzed to characterize the structure and stacking of the crystal structure. The single crystal grown on (100) is found to be fcc. The structures grown on (110) plane is found to be less dense and has no twinning directions. Further, different defect structures can be grown by creating an intentional lattice mismatch. The manipulative capabilities of colloidal epitaxy are also demonstrated by changing lattice spacing between two adjacent (100) planes. Fluorescence confocal microscopy is shown to be of immense use in determining symmetry of the layers, the defect structure resulting from intentional mismatch of the lattice spacing and the crystal structure of the large size colloidal crystals, grown using template-directed colloidal crystallization.

It may be mentioned here that colloidal crystals grown using similar procedures have been employed as templates for producing novel materials such as porous silica having uniform size pores (Velev *et al* 1997). The method of using colloidal crystals as templates for preparing porous materials yields products with highly uniform and structured pores of tunable size in the submicron region. Such microstructured porous materials have potential application in catalysis, filtering, coatings, microelectronics and elctro-optics.

4. Phase separation in polymer mixtures

If a binary mixture of two chemical components (which is homogeneous at high temperature and exhibits phase separation upon cooling below a composition-dependent coexistence temperature $T_c(x)$) is rapidly cooled from the single phase region to a temperature below the coexistence curve, but above the spinodal decomposition curve $T_s(x)$, the mixture is unstable, and rapidly separates into two spatially bicontinuous phases (Gunton *et al* 1983). Scattering techniques are useful in probing the dynamics of coarsening in this regime (Goldburg 1983; Bates and Wiltzius 1989). In the case of nucleation and growth regimes, the minority phase droplets are quite polydisperse and can have complicated morphologies. Hence it is difficult to interpret the data from scattering experiments. The conventional microscopes are also inadequate to probe this regime as these are limited by their large depth of field, which is typically much larger than the distance between droplets. On the other hand, CLSM provides answers to many questions regarding the spatial structure and coarsening dynamics of off-critical mixtures undergoing phase separation (White and Wiltzius 1995; Jinnai *et al* 1997).

It is possible to make three-dimensional, real space measurements of structure in phase separating off-critical mixtures using a fluorescent CLSM (White and Wiltzius 1995). Using this technique, they directly determined domain size distributions and spatial correlation at various coarsening times in samples with low minority phase volume fractions ($0·021 < x < 0·067$). The studied mixtures consisted of low molecular weight, low polydispersity oligomers of polystyrene (PS) and polybutadiene (PB). Very small quantity of fluorescent dye, pyrromethene 580 was used to provide contrast between the phases. Both PB-rich and PS-rich mixtures have been studied. All the PS-rich samples had 75% PS by volume and the minority phase volume fractions being $x = 0·067$, 0·040 and 0·021. The samples were allowed to coarsen for specified times (20–320 h) at the chosen quench temperature, and then frozen for imaging with a second quench to room temperature. 30–50 Optical sections separated in depth by a distance of 0·3 μm, with a lateral resolution of ~ 0·3 μm were acquired using fluorescence-CLSM, which allowed to construct 3D images of micron-size features. Each optical section was binarized by assigning each pixel a value 1 in the PS-rich matrix phase and 0 in the PB-rich droplets using the standard

techniques available for this purpose (Morgan and Seul 1995). Series of binarized sections can be recombined to form a 3D binary array representing the domain structure of the sample. This array can be used for determining both the size and location of each of the minority phase domains as well as the overall minority phase volume fraction of the sample. Using this computer analysis, White and Wiltzius (1995) calculated $F(R, t)$, the distribution of domain radii R, at coarsening times t from different PS-rich samples and also the pair-correlation function $G(r, t)$. Using $F(R, t)$ the time dependence of average domain radius $\bar{R}(t)$ could also be obtained for further analysis. Thus confocal microscopy has provided vital quantitative 3D real space structural information. Many previous studies of real space structure in phase separating metal alloy systems relied on inferring 3D structural information from isolated two-dimensional sections (Kaysser *et al* 1984; Hardy and Voorhees 1988). However, the 3D information obtained using CLSM is more accurate and reliable. White and Wiltzius (1995) obtained the scaled domain size distributions $4sf(R/\bar{R}, x)$ from CLSM measurements and compared with that calculated from models for coarsening process. Analysis showed that the data was not consistent with that expected for a coarsening by the evaporation–condensation mechanism (Lifshitz and Slyozov 1961), in which the minority phase domains grow by molecular diffusion through the majority phase. On the other hand, a good agreement was found with Smoluchowski model of coalescence (Siggia 1979; Visek 1989) according to which the scaled size distributions should be independent of x. Further, the confocal measurements on PB-rich sample confirm that the domain growth is by coalescence. Thus the quantitative analysis using CLSM reveals that in polymer mixtures with moderately low volume fractions, the coarsening occurs almost entirely by domain coalescence.

Apart from the study of nucleation and growth regime, CLSM has also found application in the investigation of polymer mixtures quenched to the spinodal region of the phase diagram (Jinnai *et al* 1997). When a polymer mixture is rapidly quenched to the spinodal region, the unstable mixture separates via spinodal decomposition into two phases and forms a bicontinuous two-phase structure, if the volume fraction of one of the phases is close to 0·5. Using scattering techniques, the earlier studies had concentrated on understanding the dynamics of spinodal decomposition including the time evolution of structural properties such as characteristic wavelength, Λ_m, of the phase-separated structure (Bates and Wiltzius 1989; Hashimoto *et al* 1991; Jinnai *et al* 1994). However, not many studies exist which estimate the Gaussian curvature of interfaces in polymer blends, microemulsions and other complex fluids. The Gaussian curvature K and the mean curvature H are two interfacial

curvatures which characterize an interface. Since the curvatures of the surface vary from point-to-point, it is better to define the area averaged mean curvature, $\langle H \rangle$, and Gaussian curvature $\langle K \rangle$ (Jinnai *et al* 1997) as

$$\langle H \rangle = \frac{1}{2} \frac{\int\int (k_1 + k_2)\, da}{\int\int da}, \qquad \langle K \rangle = \frac{\int\int (k_1 k_2)\, da}{\int\int da}, \qquad (1)$$

where da is the area element of the interface and k_1, k_2 are the principal curvatures of the interface at point of interest.

Recently small-angle-neutron scattering technique has been used to determine the curvatures of the bicontinuous structures in a microemulsion system (Lee and Chen 1994). Though scattering techniques yield information on mean curvature H, the determination of Gaussian curvature K is still found to be difficult because of large experimental errors associated with these measurements. However, recently Jinnai *et al* (1997) have shown that CLSM provides direct measurement of both the curvatures with sufficient accuracy. They used a polymer blend consisting of 50/50 wt% of polybutadiene (PB) and poly(styrene-ran-butadiene) (SBR). Anthracene was attached to PB for contrast enhancement. For details of sample preparation, refer Jinnai *et al* (1997). The sample contains the phase separated structure placed between the coverslips. The mixture was annealed at 373 K for various times t which are characteristic of late stage spinodal decomposition. They used CLSM (Carl-Zeiss LSM 410) with a 364 nm laser. Sixty image slices (256×256 pixels) with 0·5 μm increments along the optic axis of microscope (z axis), were acquired using an oil-immersed 40× objective. Each slice covered an area of 80×80 μm^2 in the xy-plane and the axial spacing between slices was 20 μm. For 3D construction of the interface, these images were subjected to 'binarization' with appropriate thresholds. From these images the phase-separated structure was identified to be bicontinuous. Further image analysis allowed the determination of quantities such as the characteristic wavelength of the interface, spatial correlation function, and by 3D Fourier transformation, the structure factor $S(Q, t)$ was derived. The mean and Gaussian curvatures of the interface could also be determined from the reconstructed 3D image using a procedure called 'parallel surface method'. Using this method, $\langle H \rangle$ and $\langle K \rangle$ values were estimated to be 0·01 μm^{-1} and $-0·062$ μm^{-2}, respectively for a sample which was annealed for 70 h. Principal curvatures $\langle k_1 \rangle$ and $\langle k_2 \rangle$ were also estimated (Jinnai *et al* 1997).

A small positive value for $\langle H \rangle$ means existence of cylindrical or spherical domains when a part of the domain breaks in the course of spinodal decomposition. The negative value of $\langle K \rangle$ implies that the interface of

the phase-separated polymer blend on the average is hyperbolic. Further, the ratio of the mean radius of curvature of the interface Λ_m to t is found to be constant with respect to t, which implies that dynamical scaling hypothesis holds in the late stage spinodal decomposition. Ribbe *et al* (1996) have shown that the methods for complex image generation in the CLSM and analysis provides information about the morphology of the polymer blend system. These experimental studies demonstrate the importance of CLSM in quantitative understanding of complex phenomenon such as phase separation in polymer mixtures.

5. Applications in technological materials

CLSM is now finding applications in investigating processes and materials of technological importance viz. evaluation of the fracture process in steels, in corrosion studies, in accurate measurement of residual strains in metal composites and semiconductor devices. This section deals with some of these applications in brief.

Recently, Enmark *et al* (1996) investigated the fracture behaviour of surface-cracked panels of tempered martensitic steels, to examine the failure conditions at temperatures corresponding to the quasi-cleavage fracture regime. Studies on tempered martensitic steels are of interest as these are being considered as structural materials for fast breeder and fusion reactors owing to their good thermomechanical properties and good swelling resistance to environments. There is also considerable interest in characterizing the ductile–brittle transition in these materials and its significance to fracture resistance of fusion reactor structures.

To study the fracture behaviour, Enmark *et al* (1996), created semi-elliptical surface cracks at the centre of one side of the tempered martensitic stainless steel specimens, which were rectangular in cross-section. The crack creation and specimen preparation are described in detail by Enmark *et al* (1996). Samples were subjected either to tension or three-point bending to achieve cracks of required dimensions. Scanning electron microscopy and confocal microscopy have been used to examine the fractured surfaces. SEM has been used to characterize the cleavage nature of the entire fracture surface and confocal microscopy to generate quantitative 3D topographic maps of the fracture surfaces. These maps in turn can be used with fracture reconstruction techniques to evaluate the values of crack tip opening displacement, δ^*, along the crack front at the time of fracture. The measured δ^* values were used to calculate an effective fracture toughness, $K_{J\delta}$, for the surface cracked panels. The effective toughness values determined from δ^* have been compared with a trend line for valid K_{JC} values determined from linear elastic fracture mechanics (LEFM) and elastic–plastic fracture mechanics tests conducted on

through crack specimens of the same material. By making such a comparison, Enmark *et al* could show that shallow surface crack specimens exhibit high effective toughness even at temperatures corresponding to quasi-cleavage fracture.

In another study, Odette *et al* (1996) determined fracture toughness as function of test temperature for V–4Cr–4Ti alloy under both static and dynamic conditions using SEM and confocal microscopy. The samples used for this study were pre-cracked charpy specimens of small size. Three-dimensional topographies of the fracture surfaces obtained using confocal microscopy were used along with fracture reconstruction methods to ascertain the sequence of events leading up to fracture and the critical crack tip opening at the point of crack initiation. Fracture reconstruction sequences have been used to show the process of material separation in the plane of the crack as function of crack opening displacement.

Materials can fail not only due to mechanical stresses leading to fracture, but also due to corrosion. Localized corrosion is known to be a major cause of degradation failure in materials of technological importance. Thus the detection of corrosion for preventive purposes and new methods for studying the corrosion process are of great practical importance. Corrosion process can be studied using several techniques. However, the experimental methods that can (i) measure corrosion rate, (ii) locate breakdown sites, and (iii) study the fundamental properties of passive films (such as the optical and electronic properties) and their relationship to the local stability of the films, are relatively few in number. In order to locate corrosion site, the entire region of the corroding surface is to be imaged for which CLSM is best suited. Confocal microscopes also provide information about all the three topics mentioned above.

Sukamoto *et al* (1995) demonstrated the optical slicing capability of CLSM by imaging a polycrystalline Cu substrate which was etched preferentially with a solution of deaerated 0.1 M H_2SO_4 and 0.1 M H_2O_2 for 30 min. A 3D image is formed by combining a series of optical slices, where an individual optical slice represents a plane of focus. The 3D image of the etched Cu surface can be shown as fish-net plot by depth coding the section series. The depth coding procedure includes finding out the maximum intensity along the z-axis for each point in the xy-plane and converting the z-position to intensity. Alternatively, xz- and yz-section scans are also possible. The xz- and yz-slice show the surface profile viewed from two perpendicular directions. In the latter mode, the CLSM becomes a noncontact surface profilometer. This surface profiling technique can also be used to produce one- and two-dimensional plots of surface topography with a sensitivity of better than 100 nm. Further, the software of CLSM can provide 3D projections of the series of optical sections. This allows to visualize

inside of the objects, e.g. pores of porous materials. Since the reflected light intensity depends on the optical properties of the medium through which the incident light traverses, it is also possible to extract from the reflected light intensity the information regarding the composition of the medium which directly affects the optical properties. This can be used to image reactant-product layers on corroding surfaces, which is similar to the use of phase detection interferometric microscope (PDIM) for refractive index mapping of concentration profiles (Sukamoto *et al* 1995). However, there are some differences. The depth resolution of the PDIM is better than that corresponding to CLSM, whereas the advantage of CLSM is that the measured intensity can be correlated directly with the vertical position.

The optical techniques discussed above allow one to monitor and determine the corrosion rate by measuring topographical changes of the surface which is in contact with environment (top surface). Topographical changes are determined from changes in the reflected light and light incident from the top. The relative etching or corrosion rates thus obtained can be converted to absolute rates by masking one part of the surface.

High depth resolution and depth discrimination property associated with CLSM, have paved the way for finding out new methods of measuring the residual fibre strains in fibre-reinforced titanium matrix composites. The method involves selectively etching the matrix over a prescribed length of a composite and subsequently measuring the extension of the relaxed fibres relative to neighbouring fibres that are still embedded within the matrix material. Ramamurthy *et al* (1996) proposed and applied this new method to fibre-reinforced metal titanium matrix composites. Figure 10 shows schematic of the specimen and its dimensions. The sample preparation involves making two narrow slits (width ~ 300 μm, length ~ 50 mm) with ~ 1 mm separation and then dissolving the matrix between the slits after masking the exposed

portion of the material within the slits. Once the matrix is dissolved the fibres undergo relaxation, and the extension, Δ, (figure 10) of the exposed fibres is measured by the heights of the tops of the fibres both in the exposed and the intact regions using CLSM. The precision involved in these measurements is about 1 μm. The residual fibre strain is obtained using the relation $\varepsilon_f = -\Delta/l$, where l is the length of the exposed fibre. Ramamurthy *et al* (1996) suggest that with the improvements in surface conditions, the precision in measuring Δ can be as high as the resolution of confocal microscope 0·2 μm. The other method used earlier involves selectively etching the matrix from a central portion of strip of composite and subsequently measuring the change in length of the fibres before and after dissolution. This can only give precision in the measurement of extension of about 2–4 μm which is one order of magnitude lower than the present method which employs CLSM. X-ray and neutron diffraction methods also have been used for estimation of residual strains (Noyan and Cohen 1987; Saigal *et al* 1992). However, the current method has an advantage over the diffraction techniques because the former involves simple test procedures, easy interpretation and analysis of the data.

Confocal microscopes allow us to form high resolution images with a depth of focus sufficiently small such that all the details which are imaged appear in focus. This suggests immediately that we can extend the depth of the focus of the microscope by adding together (integrating) the images taken at different focal settings without sacrificing the lateral resolution. The resultant image is called extended-focus image while the extended image formed using conventional microscopes are blurred and out-of-focus, whereas the confocal extended-focus image is excellent and is in focus across the entire field. An alternative to extended-focus method is auto-focus method. The auto-focus image is obtained by scanning the object axially and, instead of integrating, selecting the focus at each picture point by recording the maximum of the intensity. This method allows the use of confocal microscope as a non-contact surface profilometer and one such application was mentioned earlier while discussing the corrosion studies. Since the confocal microscopes give extended-focus and auto-focus images, these microscopes have found immense application in imaging and analyzing circuits in semiconductor device technology. Confocal microscopes are increasingly being used in very large scale integrated (VLSI) circuit metrology, which includes line width and overlay measurements (Wijnaendts-van-Resandt 1990).

Recently, Ribes *et al* (1995) demonstrated high resolution, large area photoluminescence mapping of porous silicon wafers with a confocal scanning stage microscope. A confocal scanning beam macroscope has been fabricated which images specimens up to 7·5 ×7·5 cm² in size in

(a) BEFORE DISSOLUTION   (b) AFTER DISSOLUTION
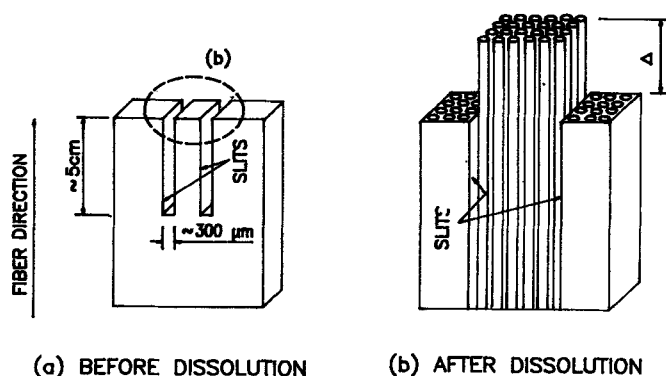
Figure 10. (a) Specimen geometry used to measure the residual fibre strain and (b) extension of exposed fibres following matrix dissolution, are shown schematically.

less than 10 s using reflected light, photoluminescence and optical beam-induced current. This instrument can also be used to evaluate preparation parameters involved in the manufacture of porous silicon as well as to provide quality control at macroscopic and microscopic levels for the fabrication of porous silicon specimens, wafers and devices.

6. Summary

Conventional optical microscopy with digital video imaging technique provides only two-dimensional information. On the other hand, CLSM has depth discrimination property, which allows one to image volume of a specimen. Since the images are acquired by scanning and the image data is available in digital form, it can be subjected to image enhancement and processing techniques without the loss of resolution. CLSM also provides capability for high resolution images using extended-focus method or auto-focus method. In the auto-focus method, CLSM acts as a noncontact surface profilometer. Since one does not need to destroy the specimens as preparative technique, confocal microscope serves as a nondestructive three-dimensional probe. TV screen is necessary to view images of scanning-stage and scanning beam confocal microscopes. However, direct viewing of a confocal image is possible using a tandem confocal microscope. Fluorescence confocal microscope offers an advantage of imaging thick biological samples in three dimensions.

While charge-stabilized suspensions having fairly large size (> 0.3 μm) particles, are turbid for light scattering studies, CLSM can probe the internal structure of such suspensions. The structural inhomogeneities, such as voids deep inside a suspension of highly charged particles, have been imaged using a CLSM. Further, the amorphous nature of disordered particle regions coexisting with voids are also characterized using frame averaging of CLSM images. These important observations provide evidence for the possibility of a gas–solid transition in a charge-stabilized suspension and presence of long-range attractive interaction in the interparticle interaction. The unusual gathering of negatively–charged colloidal particles close to the similarly-charged wall, as probed by the CLSM, provide another evidence for similar long-range attraction.

Colloidal crystals with lattice constants in the mesoscopic range are technologically important. Such applications require large single crystals. The crystals are grown usually in glass or quartz sample cells, which are small in size, and are found to have stacking disorder. It is now possible to determine the stacking disorder in such crystals using a fluorescence CLSM. Using specially designed templates, it is now possible to grow large size single crystals oriented along crystal directions without twinning. Using colloidal epitaxial process it is possible

to grow crystals with different crystal orientations next to each other by making a simple change in the spacing between adjacent planes. These structures are important for the creation of optical waveguides. Such ordered structures grown using the manipulative capabilities of colloidal epitaxy can be characterized by confocal microscopy.

The late stage of nucleation and growth process of a binary polymer mixture undergoing phase separation, where the minority phase droplets are quite polydisperse and have complicated morphologies, has been studied quantitatively using confocal fluorescence microscopy. Using this technique, it is easy to determine directly the domain size distribution and spatial correlations at various coarsening times. Further, the time evolution of a three-dimensional spatially bicontinuous structure of a polymer mixture undergoing the late stage of spinodal decomposition, has been studied and the average local geometry of the interface is evaluated directly using CLSM. Such studies greatly enhance the understanding of phase separation phenomena not only in polymer mixtures but also in complex fluids and other condensed matter systems.

Apart from probing the structure and dynamics in turbid suspensions, transparent and translucent materials, confocal microscopy has found applications in studying fracture process in martensitic steels and alloys which are very attractive candidates for structural applications in fusion reactors. Quantitative, three-dimensional topographic maps of the fracture surfaces can be generated. Fracture reconstruction sequences analyzed together with these maps allow the evaluation of the crack tip opening displacement along the crack front at the time of fracture which can be compared with finite element calculations. Such measurements and comparison with calculations throw more light in understanding the fracture process. The failure of structural component can happen not only due to the mechanical stresses but also due to corrosion, which usually occurs locally and nonuniformly. Controlling corrosion has major financial impact for industry. New techniques such as confocal microscopy helps in measuring corrosion rates and in locating the corroding sites. Since CLSM acts as noncontact surface profilometer, it is possible to do surface topography. It is also possible to measure accurately residual strain in fibre-reinforced metal composites.

Since confocal microscopy possesses a real three-dimensional response, it has been able to extend the applicability of optical methods to sub-micron metrology and inspection associated with modern semiconductor device industry. A large number of instruments are presently in use in the areas of design and development of VLSI circuits and in automatic wafer processing facilities.

From these industrial applications as well as from the results reviewed in this article it clearly emerges that

CLSM is a very useful investigative and characterizing tool to study a wide variety of materials which are of fundamental and technological importance.

Acknowledgements

References

Arora A K and Rajagopalan R 1996 in *Ordering and phase transitions in charged colloids* (eds) A K Arora and B V R Tata (New York: VCH Publishers) p. 1

Arora A K and Tata B V R 1996 in *Ordering and phase transitions in charged colloids* (eds) A K Arora and B V R Tata (New York: VCH Publishers) p. 181

Arora A K and Tata B V R 1998 *Adv. Colloid Interface Sci.* **78**

Arora A K, Tata B V R, Sood A K and Kesavamoorthy R 1988 *Phys. Rev. Lett.* **60** 2438

Asher S A, Flaugh P L and Washinger G 1986 *Spectroscopy* **1** 26

Bates F S and Wiltzius P 1989 *J. Chem. Phys.* **91** 3258

Boyde A, Jones S J, Taylor M L, Wolfe L A and Watson T F 1990 *J. Microsc.* **157** 39

Chang S, Liu L and Asher S A 1994 *J. Am. Chem. Soc.* **116** 6739

Chu X and Wasan D T 1996 *J. Colloid Interface Sci.* **184** 268

Crocker J C and Grier D G 1996a *J. Colloid Interface Sci.* **179** 298

Crocker J C and Grier D G 1996b *Phys. Rev. Lett.* **77** 1897

Dixon T 1996 *Nature* **383** 760

Dosho S *et al* 1993 *Langmuir* **9** 394

Enmark M, Edsinger K, Lucas G and Odette G R 1996 *J. Nucl. Mater.* **233** 347

Frankel D and Ladd A J C 1984 *J. Chem. Phys.* **81** 3188

Grier D G and Murray C A 1996 in *Ordering and phase transitions in charged colloids* (eds) A K Arora and B V R Tata (New York: VCH Publishers) p. 69

Goldburg W I 1983 in *Light scattering near phase transitions* (eds) H Z Cummins and P Levanyuk (Amsterdam: North-Holland)

Gunton J D, San Miguel M and Sahni P S 1983 in *Phase transitions and critical phenomena* (eds) C Domb and J L Lebowitz (New York: Academic Press) Vol. 8, p. 269

Hardy S C and Voorhees P W 1988 *Metall. Trans.* **A19** 2713

Hashimoto T, Takenaka T and Jinnai H 1991 *J. Appl. Crystallogr.* **24** 457

Howard V 1990 in *Confocal microscopy* (ed.) T Wilson (London: Academic Press) p. 285

Ilett S M, Orrock A, Poon W C K and Pusey P N 1995 *Phys. Rev.* **E51** 1344

Ise N, Ito K, Matsuoka H and Yoshida H 1996 in *Ordering*

and phase transitions in charged colloids (eds) A K Arora and B V R Tata (New York: VCH Publishers) p. 102

Ito K, Yoshida H and Ise N 1994 *Science* **263** 66

Jinnai H, Hasegawa T, Hashimoto T and Han C C 1994 *J. Chem. Phys.* **99** 4845, 8154

Jinnai H, Koga T, Nishikawa Y, Hashimoto T and Hyde S T 1997 *Phys. Rev. Lett.* **78** 2248

Kepler G M and Fraden S A 1994 *Phys. Rev. Lett.* **73** 356

Kesavamoorthy R, Babu Rao C and Tata B V R 1991 *J. Phys. Condens. Matter* **3** 7973

Kino G S and Xiao G Q 1990 in *Confocal microscopy* (ed.) T Wilson (London: Academic Press) p. 361

Larsen A E and Grier D G 1996 *Phys. Rev. Lett.* **76** 3862

Larsen A E and Grier D G 1997 *Nature* **385** 230

Lee D D and Chen S H 1994 *Phys. Rev. Lett.* **73** 106

Lekkerkerker H N W, Poon W C K, Pusey P N, Stroobants A and Warren P B 1992 *Europhys. Lett.* **20** 559

Lifshitz I M and Slyozov V V 1961 *J. Phys. Chem. Solids* **19** 35

Matsuoka H and Ise N 1993 *Chemtracts-Macromolecular Chemistry* **4** 59

Morgan N Y and Seul M 1995 *J. Phys. Chem.* **99** 2088

Muromato T, Ito K and Kitano H 1997 *J. Am. Chem. Soc.* **119** 3592

Noyan I C and Cohen J B 1987 *Residual stress measurement by diffraction and interpretation* (New York: Springer-Verlag) p. 66

Odette G R, Lucas G E, Donhue E and Sheckherd J W 1996 *J. Nucl. Mater.* **233** 502

Pusey P N and van Megen W 1986 *Nature* **320** 340

Pusey P N and van Megen W 1987 *Phys. Rev. Lett.* **59** 2083

Rajagopalan R 1996 in *Ordering and phase transitions in charged colloids* (eds) A K Arora and B V R Tata (New York: VCH Publishers) p. 339

Ramamurthy U, Dary F -C and Zok W 1996 *Acta Mater.* **44** 3397

Ribbe A E, Hashimoto T and Jinnai H 1996 *J. Mater. Sci.* **31** 5837

Ribes A C, Damaskinos S, Dixon A E, Ellis K A, Dattagupta S P and Fauchet P M 1995 *Prog. Surface Sci.* **50** 295

Saigal A, Kupperman D S and Majumdar S 1992 *Mater. Sci. Engg.* **A150** 59

Schätzel K 1996 in *Ordering and phase transitions in charged colloids* (eds) A K Arora and B V R Tata (New York: VCH Publishers) p. 17

Siggia E D 1979 *Phys. Rev.* **A20** 595

Sirota E B, Ou-Yang H D, Sinha S K, Chaikin P M, Axe J D and Fujji Y 1989 *Phys. Rev. Lett.* **62** 1528

Sood A K 1991 in *Solid state physics* (eds) H Eherenreich and D Turnbull (New York: Academic) Vol. 45, p. 1

Sogami I and Ise N 1984 *J. Chem. Phys.* **81** 6320

Sukamoto J P H, Smyrl W H, Casillas N, Al-Odan M, James P, Jin W and Douglas L 1995 *Mater. Sci. Engg.* **A198** 177

Sunkara H B, Jethmalani J M and Ford W T 1994 *Chem. Mater.* **6** 362

Tarhan I L and Watson G H 1996 *Phys. Rev. Lett.* **76** 315

Tata B V R 1992 *Phase transitions in dilute charged colloidal suspensions*, Ph. D. Thesis, University of Madras, Madras (unpublished)

Tata B V R and Arora A K 1995 *Phys. Rev. Lett.* **75** 3200

Tata B V R and Arora A K 1996 in *Ordering and phase*

transitions in charged colloids (eds) A K Arora and B V R
Tata (New York: VCH Publishers) p. 140

Tata B V R and Ise N 1996 *Phys. Rev.* **B54** 6050

Tata B V R and Ise N 1997 *Laser applications in material
science and industry* (eds) R Kesavamoorthy, A K Arora, C
Babu Rao and P Kalyanasundaram (New Delhi: Allied Pub-
lishers) p. 273

Tata B V R and Ise N 1998 *Phys. Rev.* **E** (communicated)

Tata B V R, Rajalakshmi R and Arora A K 1992 *Phys. Rev.
Lett.* **69** 3778

Tata B V R, Yamahara E, Rajamani P V and Ise N 1997a
Phys. Rev. Lett. **78** 2660

Tata B V R, Rajamani P V, Yamahara E and Ise N 1997b
Solid State Phys. (India) **C40** 345

van Blaaderen A, Ruel R and Wiltzius P 1997 *Nature* **385** 321

van Megen W 1995 *Transp. Theory Stat. Phys.* **24** 1017

van Roij R and Hansen J P 1997 *Phys. Rev. Lett.* **79** 3082

Velev O D, Jede T A, Lobo R F and Lenhoff A M 1997
Nature **389** 447

Verhaegh N A M and van Blaaderen A 1994 *Langmuir* **103**
1427

Verhaegh N A M, van Duijneveldt J S, van Blaaderen A and
Lekkerkerker H N W 1995 *J. Chem. Phys.* **102** 1416

Visek T 1989 *Fractal growth phenomena* (Singapore: World
Scientific)

White W R and Wiltzius P 1995 *Phys. Rev. Lett.* **75** 3012

Wijnaendts-van-Resandt R W 1990 in *Confocal microscopy* (ed.)
T Wilson (London: Academic Press) p. 339

Wilson T 1990 in *Confocal microscopy* (ed.) T Wilson (London:
Academic Press) p. 1

Yoshida H, Ise N and Hashimoto T 1995 *J. Chem. Phys.* **103**
10146